X-Ray Magnetic Circular Dichroism: basic concepts and applications for 3d transition metals

Stefania PIZZINI
Laboratoire Louis Néel CNRS- Grenoble

I) - Basic concepts of XAS and XMCD
- XMCD at $L_{2,3}$ edges of 3d metals

II) - Examples and perspectives

X-ray Magnetic Circular Dichroism (XMCD)

difference in the absorption of left and right circularly polarised x-rays by a magnetic material

$$XMCD = \sigma^{L} - \sigma^{R}$$

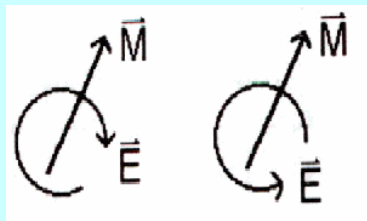

Local probe technique

→ magnetic moment of probed magnetic elements

Synchrotron radiation

- high flux
- energy tunable
- polarised
- coherent
- time structure

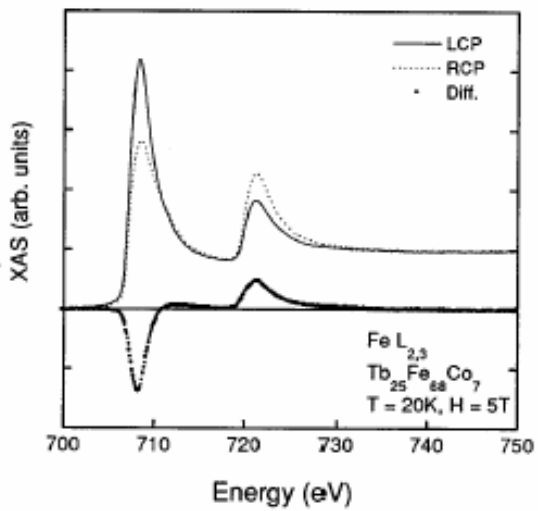

X-ray Magnetic Circular Dichroism (XMCD)

XMCD = $\sigma^{L} - \sigma^{R}$ equivalent to Faraday/Kerr effect in visible spectrum

1846 - **M. Faraday**: polarisation of visible light changes when trasmitted by a magnetic material

1975 - **Erskine and Stern** - first theoretical formulation of XMCD effect

excitation from a core state to a valence state for the $M_{2,3}$ edge of Ni.

1987 - **G. Schütz et al.** - first experimental demonstration of the XMCD at the K-edge of Fe

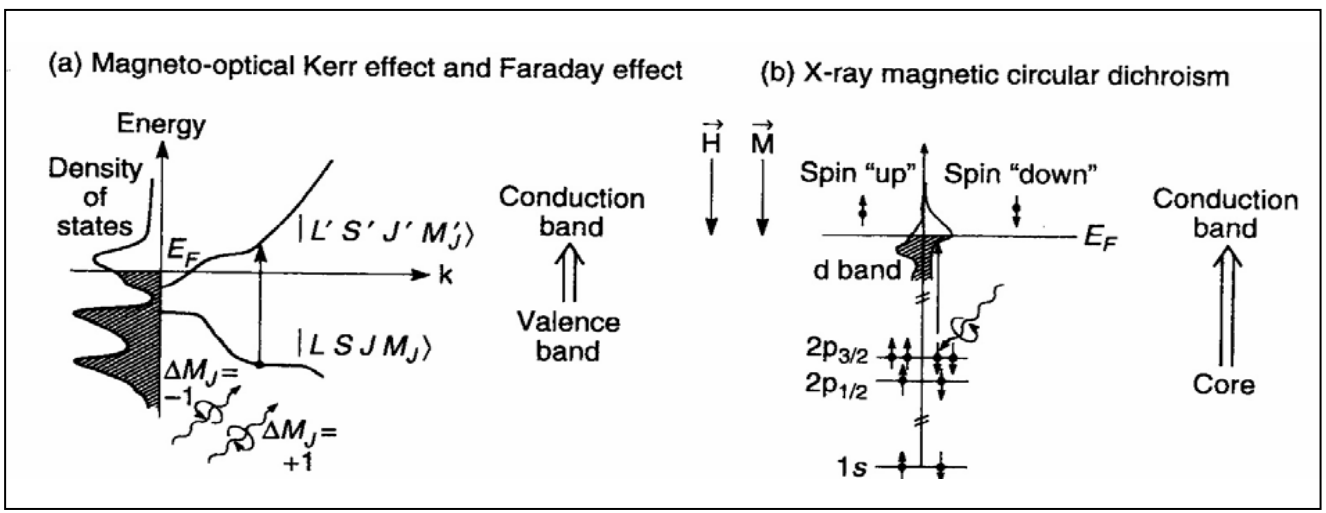

Main properties of XMCD

- **Element selectivity**

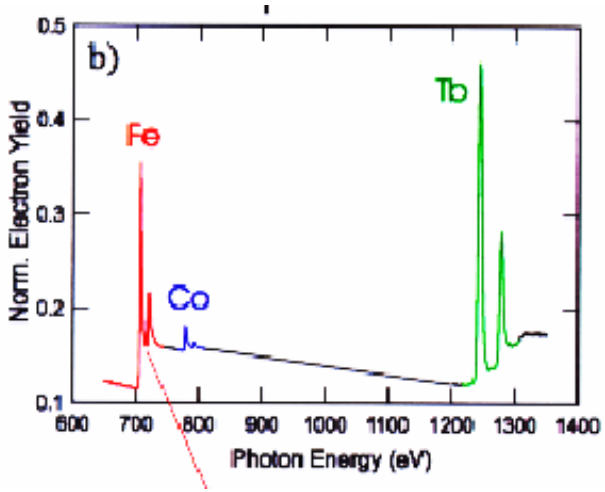

- **Orbital selectivity**

  different edges of a same element

  →different valence electrons

Fe : $L_{2,3}$ edges 2p → 3d ; K edge 1s → 4p

- **Sum rules**

  allow to obtain separately orbital and spin contributions to the magnetic moments from the integrated XMCD signal.

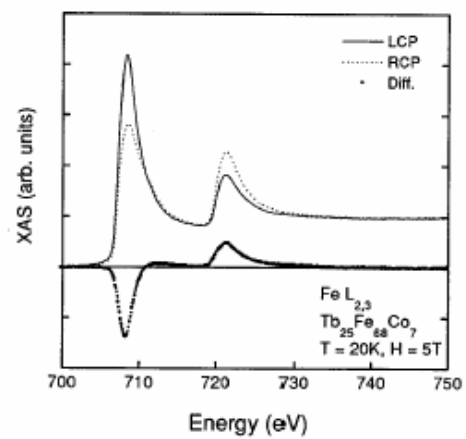

- **Sensitivity** << 1ML

- **XMCD relies on the presence of a net <M> along k. Ferromagnetic, ferrimagnetic and paramagnetic systems can be probed.**

- XMCD can be used for **element specific magnetic imaging (see Kuch lecture)**

$L_{2,3}$ edge XMCD in 3d metallic transition metals

- Magnetic 3d metals: Fe ($3d^7$), Co ($3d^8$), Ni ($3d^9$)

one-electron picture: **interaction with neigbouring atoms >> intra-atomic interactions**

→ transition of one electron from core spin-orbit split **$2p_{1/2}$, $2p_{3/2}$** level to valence **3d** band; the other electrons are ignored in the absorption process

Experimental $L_{2,3}$ edge spectra

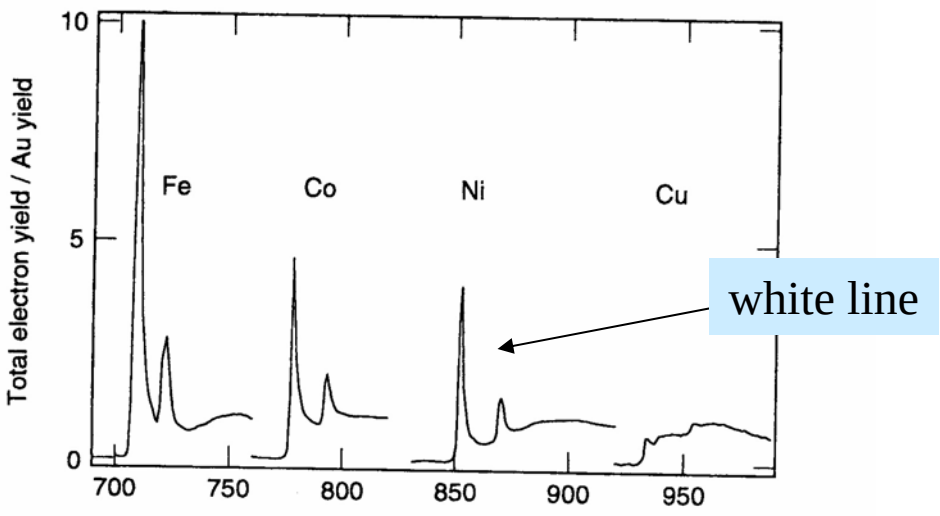

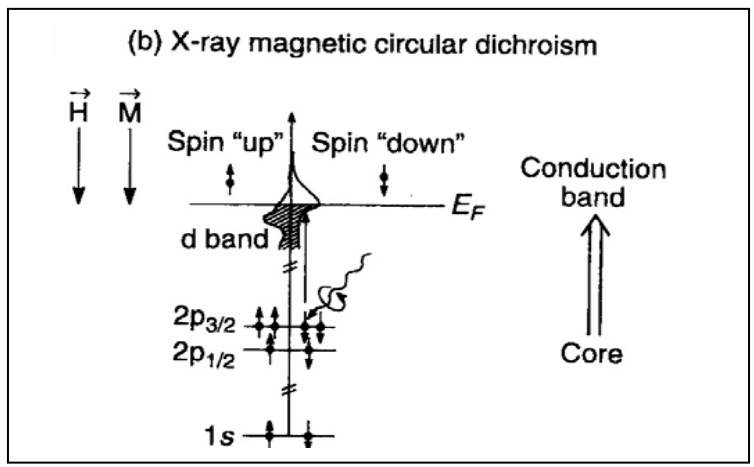

Spin -orbit coupling: $l \geq 1$
Spin parallel/anti-parallel to orbit:
$j = l + s, l - s$ $p \rightarrow 1/2, 3/2$

Here we deal with the polarisation dependence of the ' white lines '

Interaction of x-rays with matter

$$I(\omega) = I_0(\omega)\, e^{-\sigma(\omega)x}$$ Lambert-Beer law

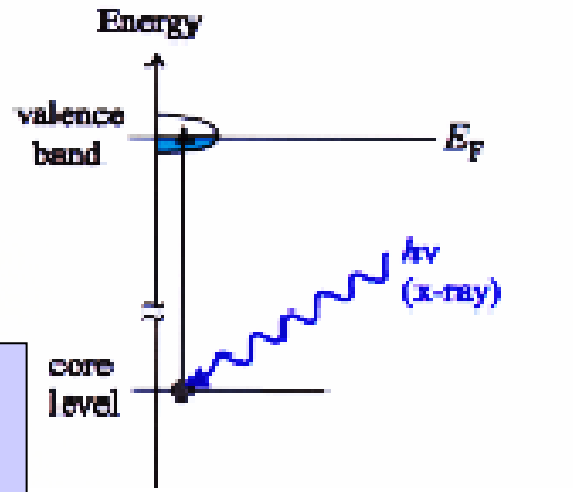

I (I_0) = intensity after (before) the sample
x= sample thickness ;
σ= experimental absorption cross section

Fermi Golden Rule

$$\sigma_q \propto \Sigma_f |< \Phi_f | \mathbf{e_q} \cdot \mathbf{r} | \Phi_i >|^2 \rho_f (h\omega - E_i)$$

$\mathbf{e_q} \cdot \mathbf{r}$ electric-dipole field operator
$|\Phi_i >$ initial *core* state; $<\Phi_f |$ final *valence* state
$\rho_f (E)$ density of valence states at $E > E_{Fermi}$
E_i core-level binding energy
$\mathbf{e_q}$: light polarization vector ; **k** : light propagation vector ; **r** and **p**: electron position and momentu

Matrix elements reveal the **selection rules:**
$\Delta s=0$ $\Delta l=\pm 1$ $\Delta m_l=+1$ (left) $\Delta m_l=-1$ (right)

$$\sigma_q \propto \Sigma_f |< \Phi_f | \mathbf{e_q} \cdot \mathbf{r} | \Phi_i >|^2 \rho (h\omega - E_i)$$

transitions from 2*p* to 3*d* band split by exchange in $3d^{\uparrow}$ and $3d^{\downarrow}$

$$|l, m_l, s, m_s> = = a_{ml}\, Y_{1,ml}\, |s, m_s>$$

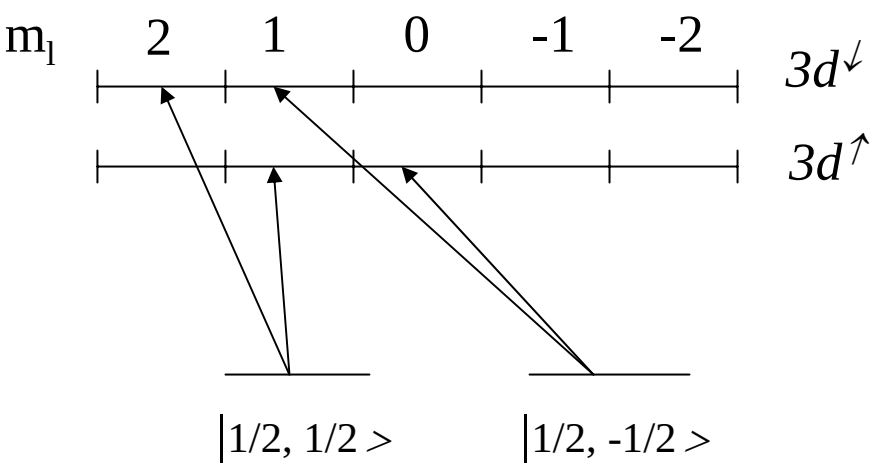

| l,s,J,m$_j$>

$|\frac{1}{2}, \frac{1}{2}\rangle$

$|\frac{1}{2}, -\frac{1}{2}\rangle$

| l,m$_l$,s,m$_s$> basis

$$-\frac{1}{\sqrt{3}} Y^{\uparrow}_{10} + \frac{\sqrt{2}}{\sqrt{3}} Y^{\downarrow}_{11}$$

$$-\frac{\sqrt{2}}{\sqrt{3}} Y^{\uparrow}_{1\text{-}1} + \frac{1}{\sqrt{3}} Y^{\downarrow}_{10}$$

L_2 edge - left polarisation (Δm_l=+1)

$\mathbf{R}=\int R_{nl}^*(r) R_{n',l'}(r)\, r^3 dr$

$$I^{\uparrow} = \sum_{i,f} |<f |P_1 |i>|^2 = (1/3\, |<2,1 |P_1 |1,0>|^2 + 2/3\, |<2,0 |P_1 |1,-1>|^2)\, R^2$$

$$I^{\downarrow} = \sum |<f |P_1 |i>|^2 = (2/3\, |<2,2 |P_1 |1,1>|^2 + 1/3\, |<2,1 |P_1 |1,0>|^2)\, R^2$$

It can be calculated (Bethe and Salpeter) that:

$|\langle 2,2 |P_1| 1,1\rangle|^2 = 2/5$
$|\langle 2,1 |P_1| 1,0\rangle|^2 = 1/5$
$|\langle 2,0 |P_1| 1,-1\rangle|^2 = 1/15$

$I^{\uparrow} = 1/3(|\langle 2,1 |\mathbf{P}_1| 1,0\rangle|^2 + 2/3 |\langle 2,0 |\mathbf{P}_1| 1,-1\rangle|^2) R^2 =$
$= (1/3 * 1/5 + 2/3 * 1/15) R^2 = 1/9\ R^2$

$I^{\downarrow} = 2/3 |\langle 2,2 |\mathbf{P}_1| 1,1\rangle|^2 + 1/3 |\langle 2,1 |\mathbf{P}_1| 1,0\rangle|^2 R^2$
$= (2/3 * 2/5 + 1/3 * 1/5) R^2 = 1/3\ R^2$

	$I^{\uparrow}$ **left**	$I^{\downarrow}$ left	$I^{\uparrow}$ **right**	$I^{\downarrow}$ right
L_2	$1/9\ R^2$	$1/3\ R^2$	$1/3\ R^2$	$1/9\ R^2$
L_3	$5/9\ R^2$	$1/3\ R^2$	$1/3\ R^2$	$5/9\ R^2$

L_2 edge

$I^{\uparrow} / (I^{\uparrow} + I^{\downarrow}) = 0.25$ LCP more $\downarrow$ states
$I^{\downarrow} / (I^{\uparrow} + I^{\downarrow}) = 0.75$

$I^{\uparrow} / (I^{\uparrow} + I^{\downarrow}) = 0.75$ RCP more $\uparrow$ states

$I^{\downarrow} / (I^{\uparrow} + I^{\downarrow}) = 0.25$

L_3 edge

$I^{\uparrow} / (I^{\uparrow} + I^{\downarrow}) = 0.625$ LCP more $\uparrow$ states

$I^{\downarrow} / (I^{\uparrow} + I^{\downarrow}) = 0.375$

$I^{\uparrow} / (I^{\uparrow} + I^{\downarrow}) = 0.375$ RCP more $\downarrow$ states
$I^{\downarrow} / (I^{\uparrow} + I^{\downarrow}) = 0.625$

→ Photoelectrons are spin-polarised

$$\sigma_q \propto \Sigma_q |< \Phi_f | e_q \cdot r | \Phi_i >|^2 \rho (h\omega - E_i)$$

For Ni, Co metal (strong ferromagnets): only empty $\rho\downarrow$

L_2 **total abs** $(I^{\downarrow}$ left + $I^{\downarrow}$ right) $\propto (1/3 + 1/9)\ R^2 =$ **$4/9R^2$**

L_3 **total abs** $(I^{\downarrow}$ left + $I^{\downarrow}$ right) $\propto (1/3 + 5/9)\ R^2 =$ **$8/9\ R^2$**

branching ratio L_3: L_2 = 2 : 1

L_2 **XMCD** $(I^{\downarrow}$ left - $I^{\downarrow}$ right) $\propto (1/3 - 1/9)\ R^2 =$ **$2/9\ R^2$**

L_3 **XMCD** $(I^{\downarrow}$ left - $I^{\downarrow}$ right) $\propto (1/3 - 5/9)\ R^2 =$ **$-2/9\ R^2$**

branching ratio XMCD $\Delta L_3 : \Delta L_2 = 1 : -1$

In general: XMCD = $(I^{\uparrow \text{left}} \rho\uparrow + I^{\downarrow}$ left $\rho\downarrow) - (I^{\uparrow \text{right}} \rho\uparrow + I^{\downarrow}$ right $\rho\downarrow)$

$= (\rho\uparrow - \rho\downarrow)\ (I^{\uparrow \text{left}} - I^{\downarrow}$ left $)$

XMCD $\neq 0$ if $\rho\uparrow \neq \rho\downarrow$

Two-step model (Wu and Stöhr)

Step 1 : spin-polarised electrons emitted by the spin-orbit split 2p band

75% spin down and 25% spin up electrons at the $\mathbf{L_2}$-edge with LCP light

37.5% spin down and 62.5% spin up electrons at the $\mathbf{L_3}$-edge with LCP light

Step 2: spin-polarised electron are analysed by the exchange split *d*-band which acts as spin-detector.

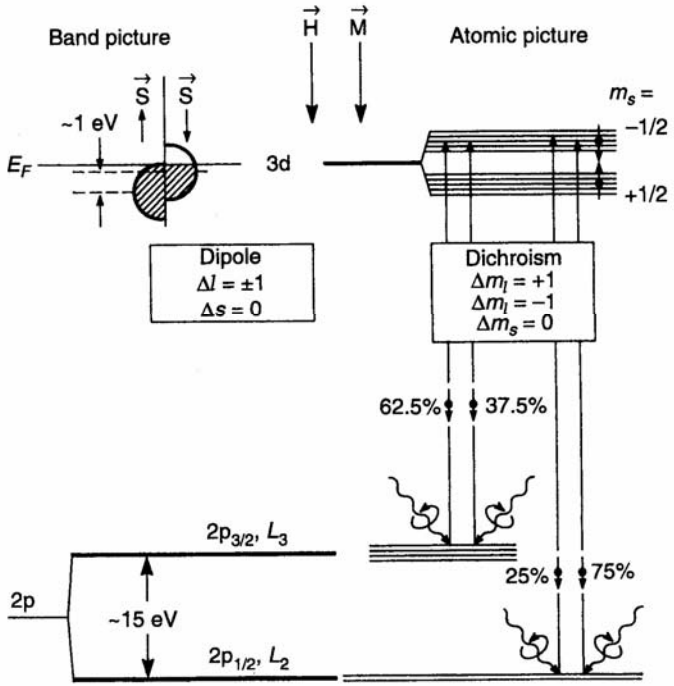

Spin-orbit splitting in *d*-band

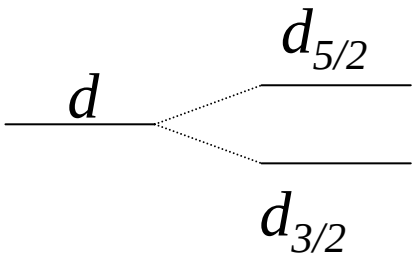

$2p_{3/2} \rightarrow 4d_{3/2,\,5/2}$

$2p_{1/2} \rightarrow 4d_{3/2,\,5/2}$

- Intensity shift from L_2 to L_3 edge $\rightarrow$ $L_3 : L_2 \geq 2 : 1$

- for XMCD there is departure from the $\Delta L_3 : \Delta L_2 = 1 : -1$; the integrated XMCD signal is proportional to the orbital moment in the 3d band.

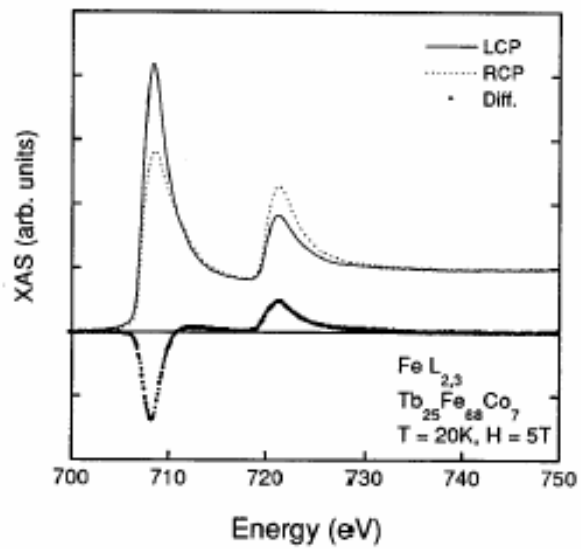

B.T.Thole and G.v.d.Laan, Europhys.Lett. 4, 1083 (1987)

Sum rules of XMCD

Sum rules relate XMCD and total absorption to the ground-state orbital and spin magnetic moment of the probed element and shell:

$L_{2,3}$-edges of Fe $\rightarrow$ Fe 3*d*-moments

Orbital moment sum rule

$$\langle L_Z \rangle = [2l(l+1)(4l+2-n)]/[l(l+1)+2 - c(c+1)] \bullet$$

$$[\int_{j+ + j-} d\omega (\mu^+ - \mu^-) / \int_{j+ + j-} d\omega(\mu^+ + \mu^- + \mu^0)]$$

l = orbital quantum number of the valence state,
c = orbital quantum number of the core state,
n = number of electrons in the valence state

μ^+ (μ^-) = absorption spectrum for left (right) circularly polarized light.

μ^0 = absorption spectrum for linearly polarized light, with polarization parallel quantization axis.

j^+ (j^-) = (l + 1/2) resp. (l - 1/2) absorption (ex. $2p_{3/2}$, $2p_{1/2}$)

B.T.Thole *et al.*, Phys.Rev.Lett. 68, 1943 (1992)
M.Altarelli, Phys.Rev.B 47, 597 (1993)

Sum rules of XMCD

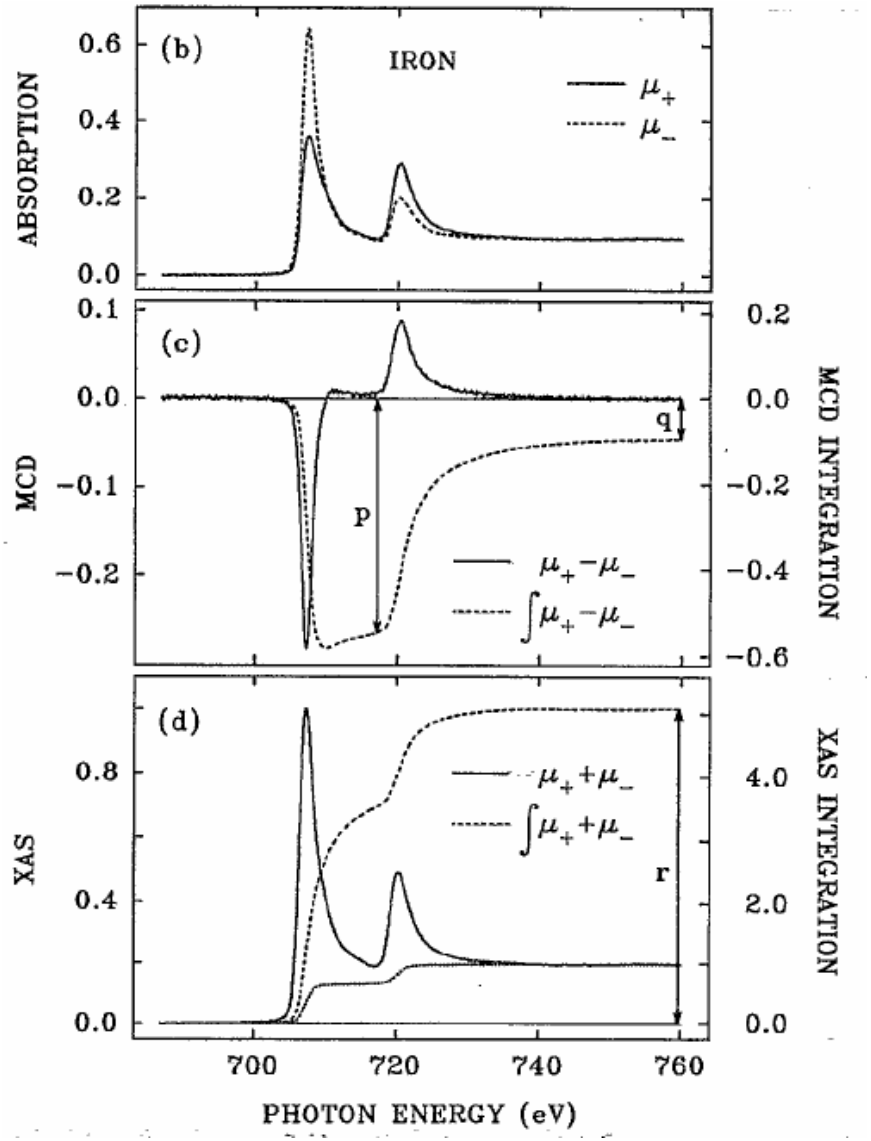

C.T.Chen *et al.*, PRL 75, 152 (1995)

For $L_{2,3}$-edges $c = 1$ ($2p$), $l = 2$ (d):

$$\langle L_Z \rangle = 4(10-n)\ (\Delta L_3 + \Delta L_2)\ /3 \int_{L3+L2} d\omega\,(\mu^+ + \mu^-)]$$

$$q = \Delta L_3 + \Delta L_2$$

$$r = \mu^+ + \mu^-$$

$$\langle L_Z \rangle = 4\,(10-n)\,q/\,3r$$

Sources of errors:

- determination of the background
- rate of circular polarization
- number of electrons *n*

Sum rules of XMCD

Spin moment sum rule

$$\langle \mathbf{S_Z} \rangle + c_2(n) \langle \mathbf{T_z} \rangle = c_1(n)[\int_{j+} d\omega\,(\mu^+ - \mu^-) - [(c+1)/c] \int_{j-} d\omega\,(\mu^+ - \mu^-)] / \int_{j+ + j-} d\omega\,(\mu^+ + \mu^- + \mu^0)]$$

$c_1(n) = 3c(4l + 2 - n)/[l(l+1) - 2 - c(c+1)]$

$c_2(n) = \{l(l+1)[l(l+1)+2c(c+1)+4]-3(c-1)^2(c+2)^2\} / 6lc(l+1)(4l+2-n)$

$\langle T_Z \rangle$ = expectation value of magnetic dipole operator

$$\mathbf{T} = \mathbf{S} - \mathbf{r}\,(\mathbf{r} \bullet \mathbf{s}) / r^2$$

which expresses the anisotropy of the spin moment within the atom

For $L_{2,3}$-edges:

$$\langle \mathbf{S_Z} \rangle + (7/2) \langle T_Z \rangle = (3/2)(10-n)[(\Delta L_3 - 2\Delta L_2)/ \int_{L3+L2} d\omega\,(\mu^+ + \mu^- + \mu^0)]$$

Sum rules of XMCD

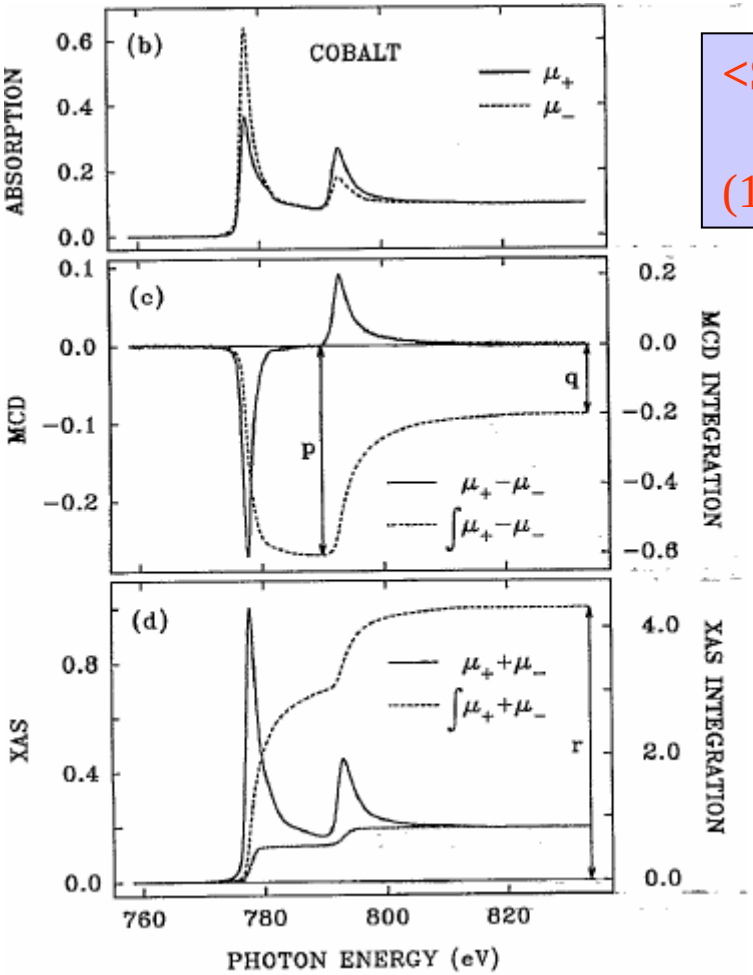

$\langle S_Z \rangle + (7/2) \langle T_Z \rangle =$

$(10\text{-}n)\ [(\Delta L3 - 2\Delta L2) / \int_{L3+L2} d\omega\ (\mu+ + \mu -)]$

$= (10\text{-}n)\ (p - 2\ (q - p))\ /\ r =$

$= (10\text{-}n)\ (3p - 2q)\ /\ r$

C.T.Chen *et al.*, PRL 75, 152 (1995)

The magnetic dipole operator T

An anisotropy of the spin moment (magnetic dipole) can be induced either by:

- anisotropic charge distribution (quadrupole moment)

  zero in cubic systems (isotropic charge)
  enhanced at surfaces and interfaces

- spin-orbit interaction

  small in 3*d* - metals
  larger in 4d and 5d metals .

Summary

-XMCD is an element selective probe of localised magnetic moments

- Sum rules allow to obtain separately orbital and spin contributions to the magnetic moments from the integrated XMCD signal.

Some applications of XMCD to the study of thin films magnetisation

Used properties:
- element selectivity
- very high sensitivity
- sensitivity to orbital and spin magnetisation
- time structure

-element-selective hysteresis loops

-induced magnetic polarisation across magnetic interface:
Pd in Pd/Fe

- microscopic origins of perpendicular magnetic anisotropy:
anisotropy of orbital moment probed by XMCD:
from thin films to single adatoms

- Recent developments: time resolved XMCD and X-PEEM

Experimental details given by Kuch

Element specific magnetic hysteresis as a means for studying heteromagnetic multilayers

C.T. Chen et al. PRB 48 642 (1993)

- Fe/Cu/Co ML evaporated on glass
- Spectra fluorescence yield

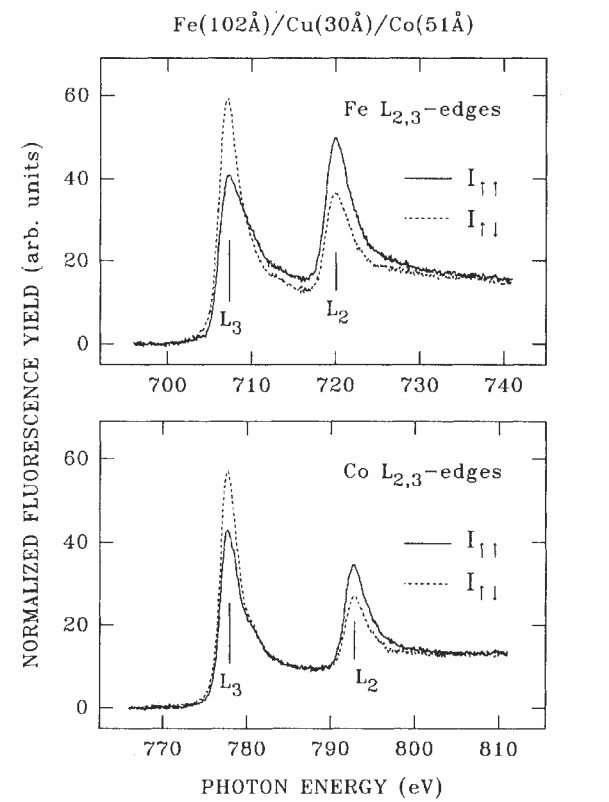

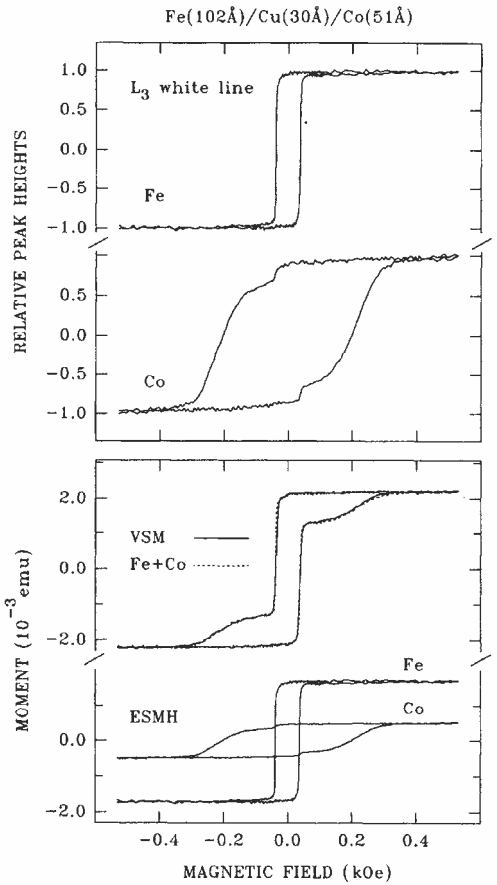

- XMCD α magn. moment
- White line ampl vs H α hysteresis loop

- Fe, Co partly coupled
- VSM as linear combination of Co and Fe cycles
  Co $1.2\mu_B$ Fe $2.1\mu_B$

Induced polarisation of 4d element across a magnetic interface in Pd/Fe multilayers

J. Vogel et al. PRB 55, 3663 (1997)

(Fe,Co,Ni)-Pd systems:

- interesting properties due to 3d-4d hybridization and exchange interactions

- Pd orders ferromagnetically when alloyed with magnetic impurities
- giant Pd moments have beeen suggested
- Co/Pd : perp. anisotropy for thin Co layers; Fe/Pd always in-plane magnetisation

- first direct determination of Pd moments by XMCD at the Pd $L_{2,3}$ edges

- Pd(X) / Fe(8 ML) with X=2,4,8,14 ML on MgO(001)

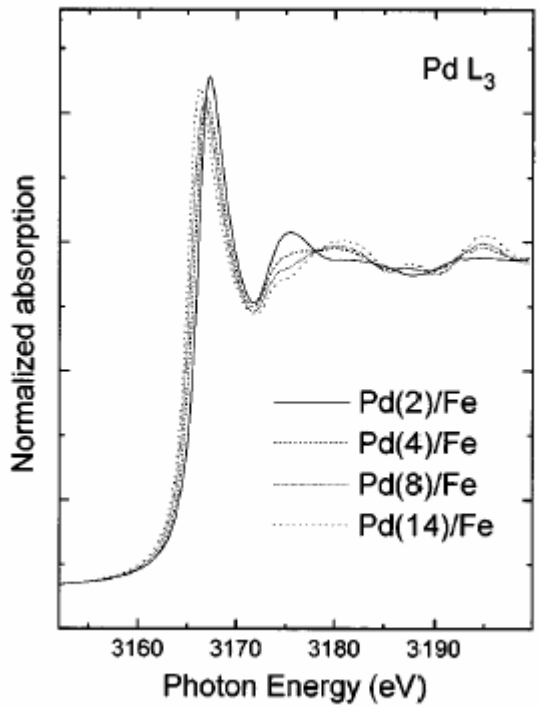

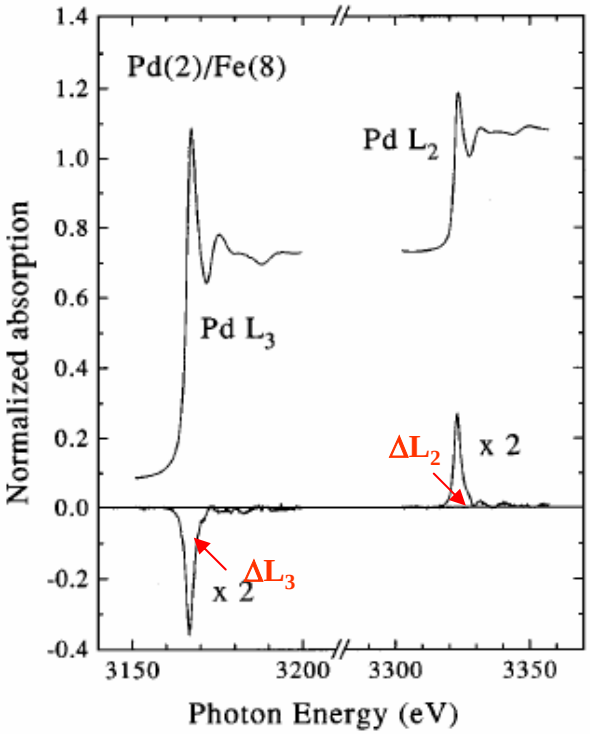

Sum rules:

$\langle L_Z \rangle = 2 \bullet (\Delta L_3 + \Delta L_2) \bullet (n_{4d} / \sigma_{tot})$

$\langle S_Z \rangle = 1.5 \bullet (\Delta L_3 - 2\,\Delta L_2) \bullet (n_{4d} / \sigma_{tot})$

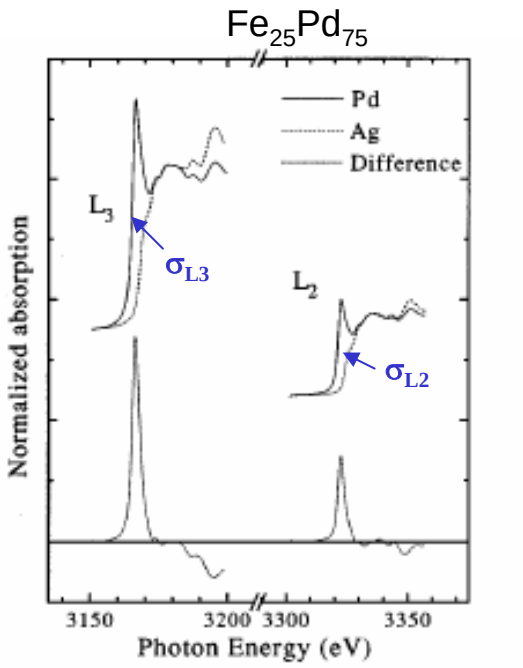

$\sigma_{L3} + \sigma_{L2} = \sigma_{tot}$

$n_{4d}(Pd) - n_{4d}(Ag) = 1.27-0.35=0.92$

	$\langle L_z \rangle$ (μ_B)	$\langle S_z \rangle$ (μ_B)	Total moment (μ_B)
Pd(2 AL)/Fe(8 AL)	0.04±0.01	0.17±0.04	0.38±0.08
Pd(4 AL)/Fe(8 AL)	0.02	0.15±0.03	0.32±0.06
Pd(8 AL)/Fe(8 AL)	0.02	0.12±0.03	0.27±0.06
Pd(14 AL)/Fe(10 AL)	0.01	0.07±0.02	0.15±0.04

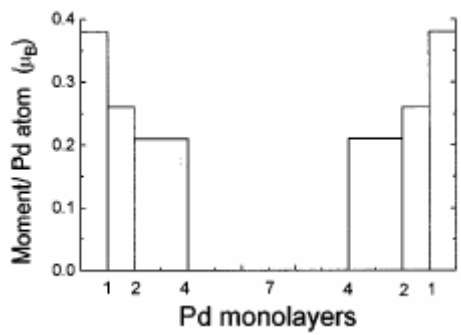

Enhanced orbital moment on Co atoms in Co/Pd multilayers

Wu, Stohr et al. PRL 69, 2307 (1992)

$L_3 / L_2 = -1.7$ $L_3 / L_2 = -2.6$

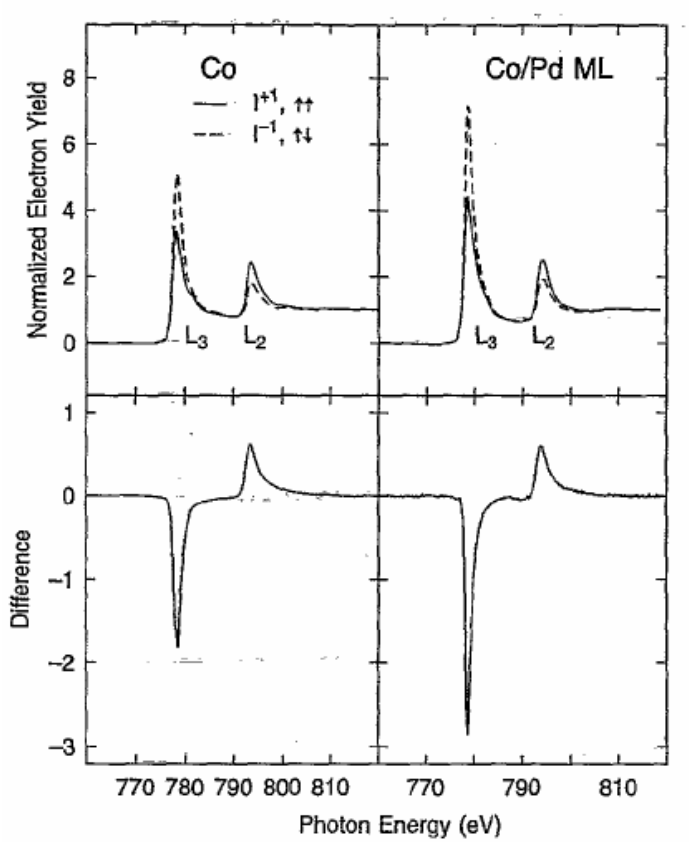

Co film $\langle Lz \rangle = 0.17 \pm 0.04\ \mu_B$

Co/Pd $\langle Lz \rangle = 0.24 \pm 0.04\ \mu_B$

First experimental confirmation of enhanced orbital moments in multilayers w.r. to pure metals

Microscopic origin of perpendicular magnetic anisotropy : orbital moment anisotropy

Weller, Stohr et al. PRL 75, 3752 (1995)

PMA arises from magnetocrystalline anisotropy (MCA) (symmetry breaking and strain at the interface)

$\Delta E_{so} \propto - \xi (m_{orb}^{\perp} - m_{orb}^{\parallel})$ Bruno PRB 39, 865 (1989)

first experimental demonstration of orbital moment anisotropy

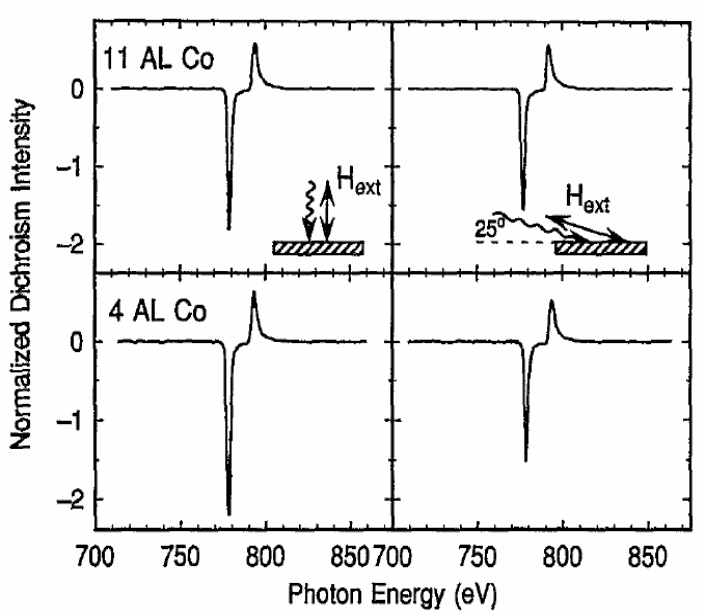

Au/Co/Au wedge

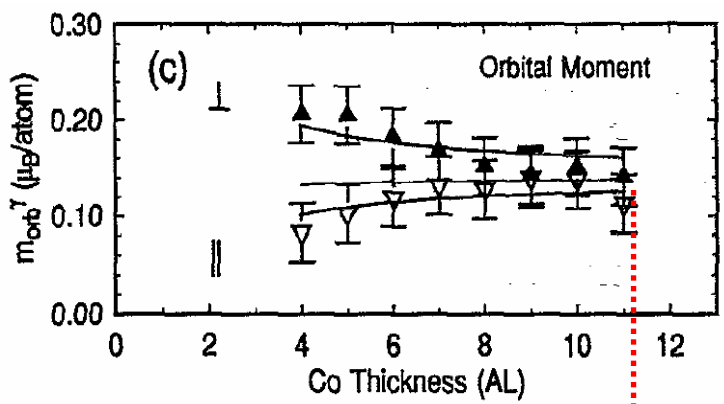

M out-of-plane **M in-plane**

Giant magnetic anisotropy of single cobalt atoms and nanoparticles

P. Gambardella *et al*. (EPF Lausanne) S. Dhesi (ESRF) Science 300, 1139 (2003)

- single Co adatoms and particles MBE deposited on Pt(111) surfaces
- a decrease of spin moment and quench of orbital moment due to crystal field is expected to be reduced in adatoms and small particles (decreased coordination)
- the high sensitivity of XMCD is used to probe magnetic anisotropy and the anisotropy of Co orbital moment

STM image of isolated Co adatoms (8.5nm x 8.5nm)

Large difference of in-plane and out-of-plane magnetisation : very large MAE

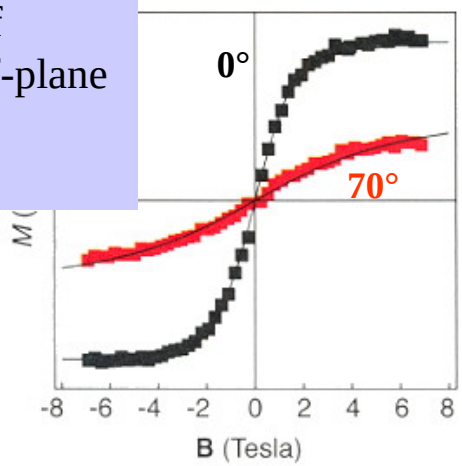

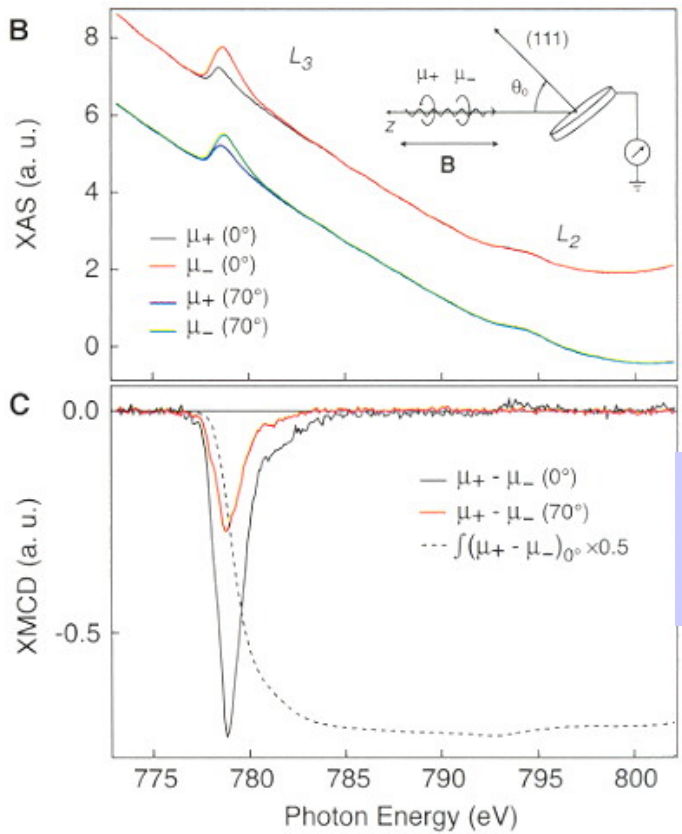

Co $L_{2,3}$ XAS spectra for 0° and 70°

vanishing L_2 XMCD very large orbital magnetism

From sum rules with n_d=2.4:

<L>=1.1 ± 0.1 μ_B for isolated Co adatoms (L=0.15 μ_B Co-hcp)
(L=0.29 μ_B 1ML Co/Pt)

very large orbital moment due to reduced coordination of the isolated Co on top of a flat surface, which favours d-electron localisation and atomic character of 3d orbitals

From element-selective XMCD magnetisation curves (up to 7 Tesla):
very large magnetic anisotropy energy (MAE)

K = 9.3 ±1.6 meV/atom (K= 1.8 meV/Co atom in $SmCo_5$)
(K=0.3 meV/atom in Pt/Co multilayers)

Effects contributing to increased MAE:
(i) Broken symmetry of Co adatoms
(ii) 3d localisation (band narrowing) →increase of s.o. energy
(iii) Additional MAE from Pt

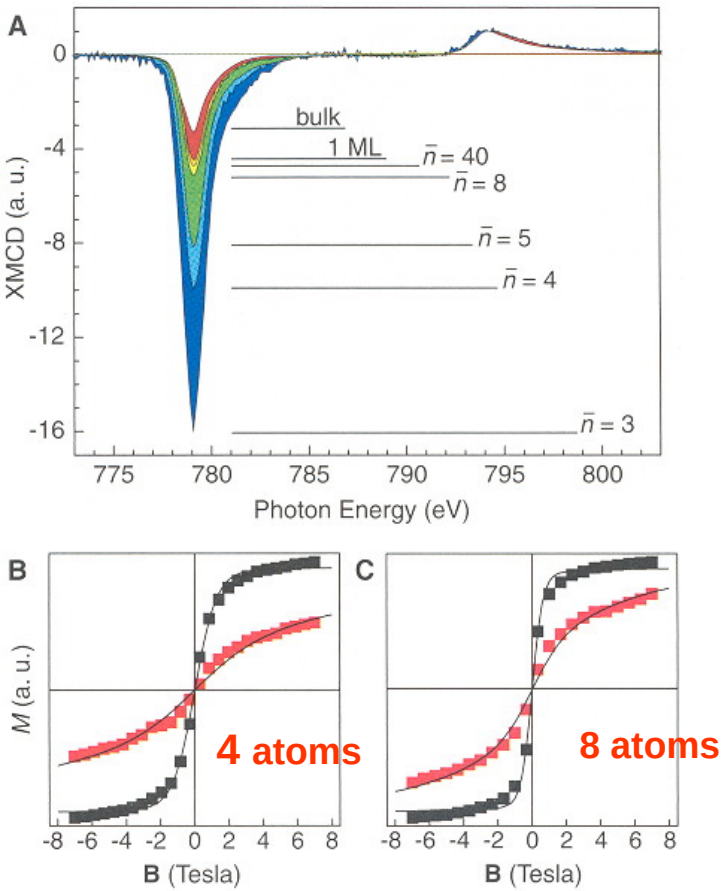

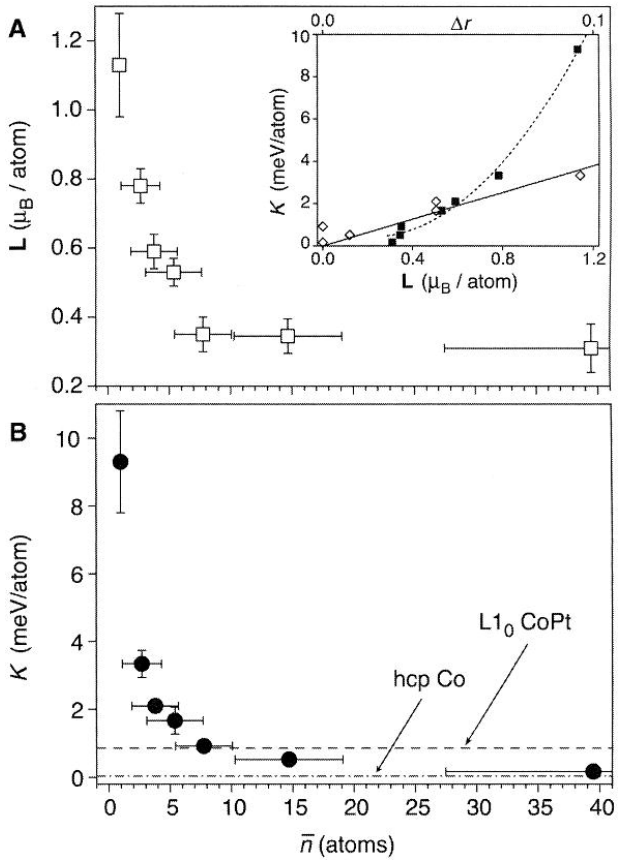

Increase of particle size : progressive quenching of orbital moment and consequent decrease of MAE

Use of the temporal structure of synchrotron radiation to study element selective magnetisation dynamics by XMCD

ESRF "single bunch" mode

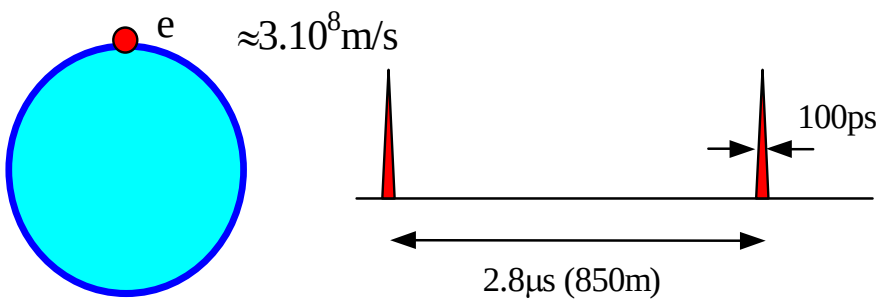

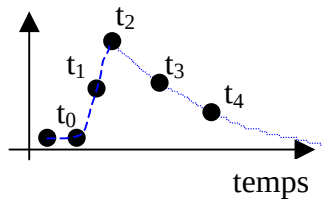

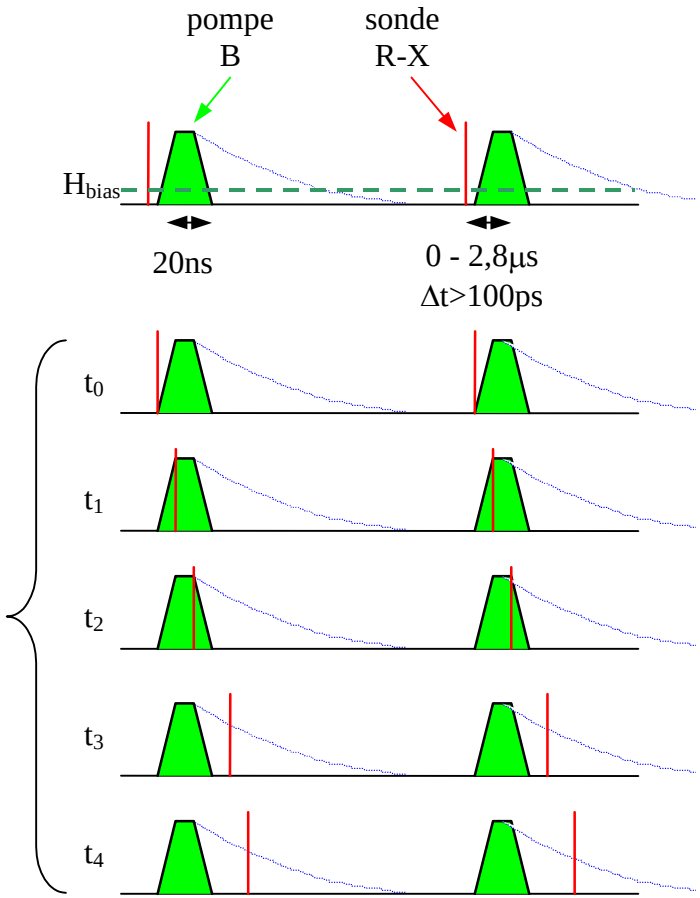

Pump-probe mode:

- Pump : magnetic pulse (microcoil)
- Probe : X-ray bunch in single bunch mode
- reproducibility : initial state needs to be the same before each pulse
- Time resolution : 100 ps in a window of 2,8 µs

M. Bonfim et al.
Phys. Rev. Lett. 86 (2001) 3646

Co(5nm)/Cu(x)/$Fe_{20}Ni_{80}$(5nm) spin valves x=6nm, 8nm, 10nm

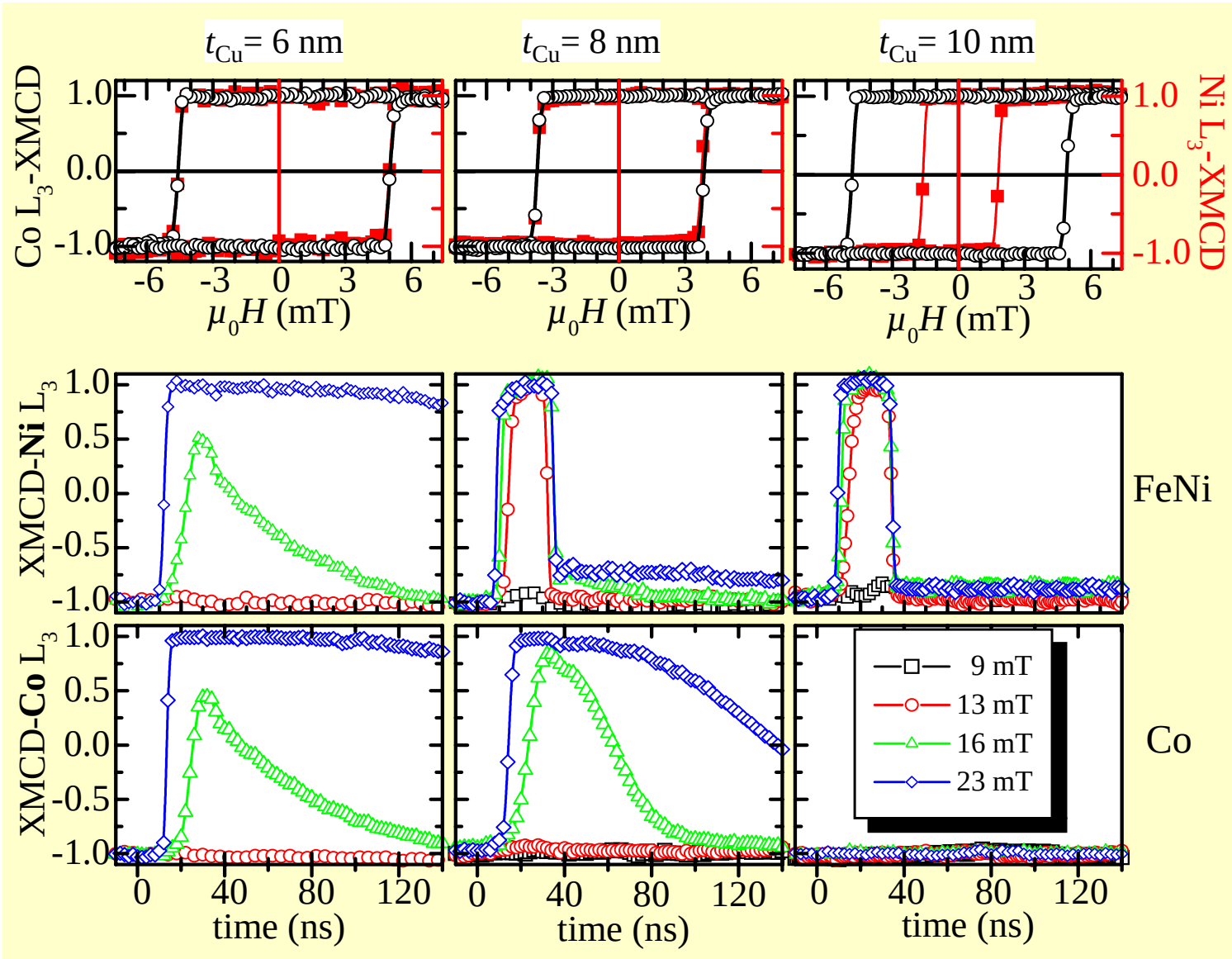

M. Bonfim et al. Phys. Rev. Lett. 86 (2001) 3646

X ray Photo Emission Electron Microscope (X-PEEM)

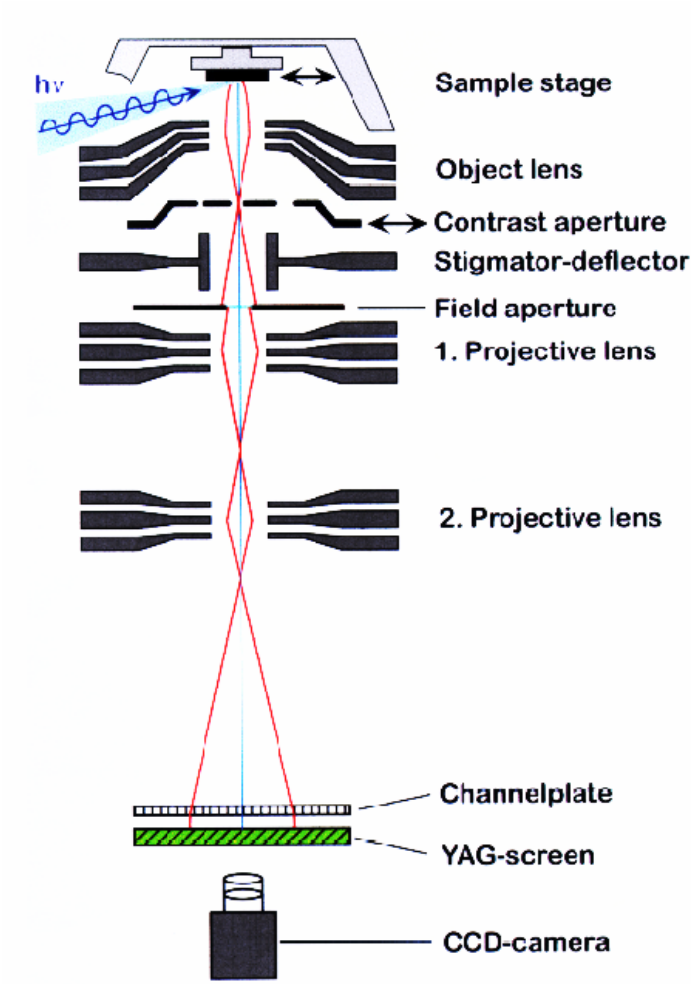

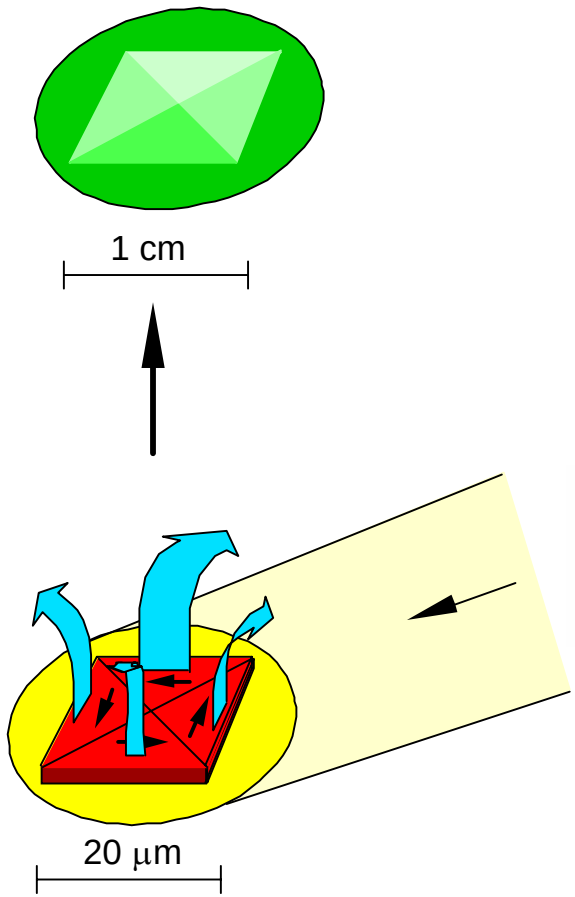

BESSY

XMCD

- **spatial resolution: < 30 nm**
- **element selectivity**
- **sensitivity: down to 1 ML**

Time-resolved X-PEEM measurements

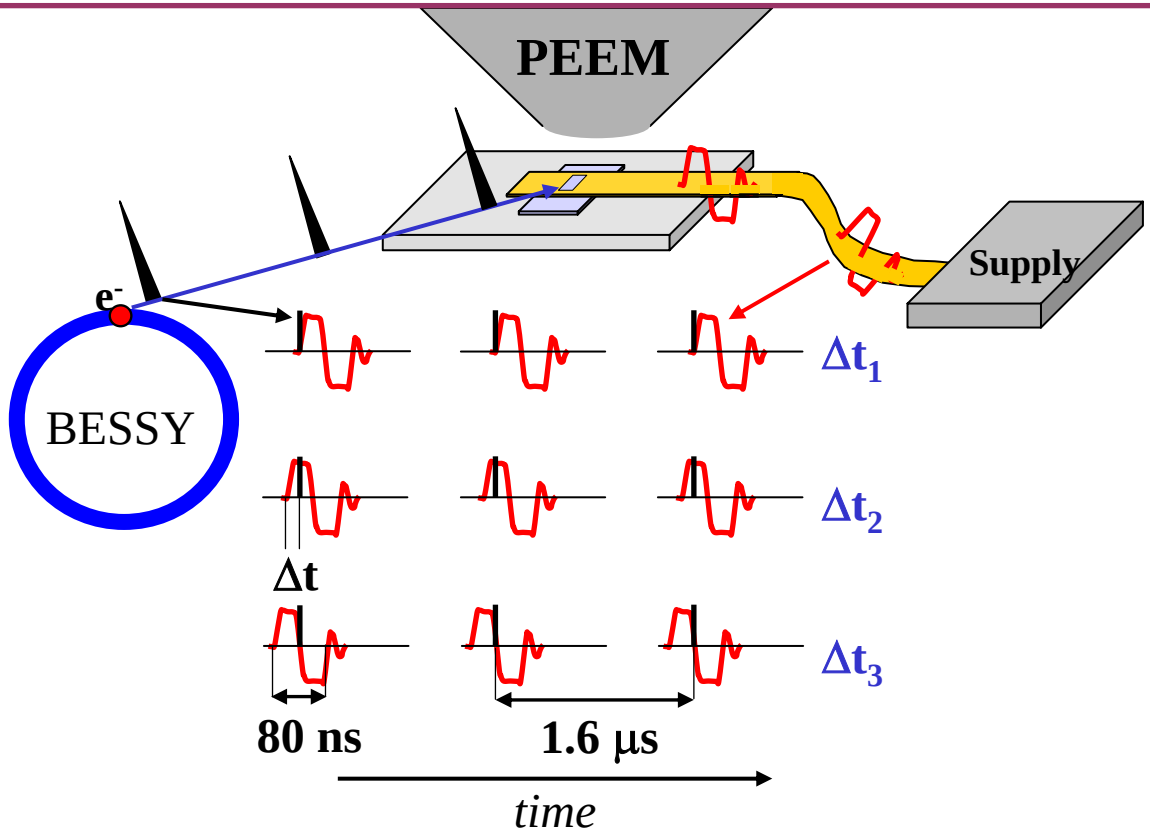

- Magnetic pulses synchronized with photon pulses.

- Domain structure as a function of field/time imaged changing delay between magnetic and photon pulses

Time resolution < 100 ps (x-ray pulse width)

Summary

element selectivity, very high sensitivity and sensitivity to orbital and spin magnetisation of XMCD

can used to obtain information on :

- element selective hysteresis
- magnetic couplings
- polarisation of non magnetic species
- orbital moment enhancement at interfaces
- anisotropy of orbital moments

in thin films systems, small particles down to single atoms.

Recent developments of XMCD have added time-resolution (TR-XMCD) and spatial resolution (X-PEEM).